Carbohydrate Polymers 84 (2011) 231–238

Contents lists available at ScienceDirect

Carbohydrate Polymers

journal homepage: www.elsevier.com/locate/carbpol

Adsorption of food dyes onto chitosan: Optimization process and kinetic

G.L. Dotto, L.A.A. Pinto*

Unit Operation Laboratory, School of Chemistry and Food, Federal University of Rio Grande – FURG, Rio Grande, RS, Brazil

ARTICLE INFO

Article history:
Received 5 October 2010
Received in revised form
10 November 2010
Accepted 11 November 2010
Available online 19 November 2010

Keywords:
Acid blue 9
Adsorption capacity
Elovich model
Food dye
Food yellow 3

ABSTRACT

Adsorption of food dyes acid blue 9 and food yellow 3 onto chitosan was optimized. Chitosan was obtained from shrimp wastes and characterized. A full factorial design was used to analyze the effects of pH, stirring rate and contact time in adsorption capacity. In the optimal conditions, adsorption kinetics was studied and the experimental data were fitted with three kinetic models. The produced chitosan showed good characteristics for dye adsorption. The optimal conditions were: pH 3, 150 rpm and 60 min for acid blue 9 and pH 3, 50 rpm and 60 min for food yellow 3. In these conditions, the adsorption capacities values were 210 mg g^{-1} and 295 mg g^{-1} for acid blue 9 and food yellow 3, respectively. The Elovich kinetic model was the best fit for experimental data and it showed the chemical nature of dyes adsorption onto chitosan.

1. Introduction

Chitosan, a de-N-acetylated analog of chitin, is a heteropolysaccharide consisting of linear b-1,4-linked GlcN and GlcNAc units (Harish Prashanth & Tharanathan, 2007). Due to properties such as, biocompatibility and biodegradability, chitosan is used in a wide range of applications, including effluent treatment (Srinivasan & Viraraghavan, 2010). The use of chitosan for dye removal from effluent is based on three factors: First, due to the fact that the chitosan-based polymers are low-cost materials obtained from natural resources and their use as biosorbents is extremely cost-effective. Second, the adsorption capacities are high and higher adsorption rates are found. The third factor is the development of complex materials by chitosan (Crini & Badot, 2008).

Over a hundred thousand commercially available dyes exist and more than 7×10^5 tons are produced annually (Elwakeel, 2009), consequently, large quantities of dyes are emitted into effluents from various industries, for example the textile and food industries (Piccin, Vieira, Gonçalves, Dotto, & Pinto, 2009). The colored dye effluents are considered to be highly toxic to the aquatic biota and affect the symbiotic process by disturbing the natural equilibrium by reducing photosynthetic activity and primary production due to the colorization of water (Gupta & Suhas, 2009). It is rather difficult to treat dye effluents because of their synthetic origins and their mainly aromatic structures, which are biologically non-degradable (Srinivasan & Viraraghavan, 2010). Adsorption is found a good way to treat industrial waste effluents, it has significant advantages in comparison with conventional methods, especially from economical and environmental viewpoints (Crini & Badot, 2008; Gupta & Suhas, 2009; Li et al., 2010; Shimei, Jingli, Ronglan, & Jide, 2006; Srinivasan & Viraraghavan, 2010).

Many studies have been developed on dyes adsorption onto alternative adsorbents, for example, reactive red 141 (Sakkayawong, Thiravetyan, & Nakbanpote, 2005); reactive black 5 (Elwakeel, 2009); acid green 25 (Gibbs, Tobin, & Guibal, 2003); acid orange 10, acid red 73 and acid green 25 (Cheung, Szeto, & McKay, 2009); methyl orange (Li et al., 2010); basic green 4 (Shimei et al., 2006) and methylene blue (Han et al., 2010). Most of dye adsorption studies are relative to textile dyes (Chatterjee, Chatterjee, Chatterjee, & Guha, 2007; Han et al., 2010; Sakkayawong et al., 2005; Shimei et al., 2006; Uzun, 2006), whereas, food dyes are little investigated. In addition, dye adsorption onto chitosan is commonly studied through kinetic and thermo chemical analysis, and a full factorial design is rarely used.

The present study aimed to produce chitosan with appropriate characteristics for dyes adsorption and to optimize adsorption of the food dyes acid blue 9 and food yellow 3 onto chitosan in batch systems. In the optimal conditions, it was verified adsorption kinetic. The effects of factors such as pH, stirring rate and contact time on adsorption capacity were investigated through surface response methodology. Adsorption kinetic were evaluated according to adsorption reaction models. In addition, scanning electron microscopy (SEM) and energy dispersive X-ray spectroscopy (EDS) were used to compare the adsorption behavior of both dyes.

* Corresponding author at: Unit Operation Laboratory, School of Chemistry and Food, Federal University of Rio Grande – FURG, 475 Engenheiro Alfredo Huch Street, 96201-900 Rio Grande, RS, Brazil. Tel.: +55 53 3233 8648; fax: +55 53 3233 8745.
E-mail address: dqmpinto@furg.br (L.A.A. Pinto).

0144-8617/$ – see front matter © 2010 Elsevier Ltd. All rights reserved.
doi:10.1016/j.carbpol.2010.11.028

2. Material and methods

2.1. Chitosan production methodology

The adsorbent used in this work was a chitosan powder, obtained from shrimp (*Farfantepenaeus brasiliensis*) wastes. Firstly, chitin was obtained by demineralization, deproteinization and deodorization steps. Chitosan paste was obtained by alkaline deacetylation of chitin followed by purification according to Weska, Moura, Batista, Rizzi, and Pinto (2007). Chitosan paste was dried to obtain a chitosan powder (Halal, Moura, & Pinto, 2010).

2.2. Chitosan characterization

Chitosan powder was characterized according to molar weight (M_w), deacetylation degree (%DD), particle size (D_p) and infrared ray analysis (FT-IR). Scanning electron micrographs (SEM) and energy dispersive X-ray spectroscopy (EDS) were carried out with chitosan before and after the adsorption process.

Chitosan molar weight was determined by viscosimetric method. Reduced viscosity was determined by Huggins equation, and converted in molar weight through Mark–Houwink–Sakurada equation (Eq. (1)) (Zhang & Neau, 2001):

$$\eta = KM_W^{\alpha} \quad (1)$$

where η is intrinsic viscosity ($mL\,g^{-1}$), M_w is molar weight (Da), $K = 1.81 \times 10^{-3}\ mL\,g^{-1}$ and $\alpha = 0.93$ (Zhao, Zhang, & Zeng, 2003).

The grain-size analysis of the chitosan powder was carried out in a standardized mesh screen. The average diameter was calculated by the Sauter definition (Foust, Wenzel, Clump, Maus, & Andersen, 1980) (Eq. (2)):

$$\overline{D}_{Sauter} = \frac{1}{\sum(\Delta X_i / D_{mi})} \quad (2)$$

where D_{Sauter} is the average diameter of Sauter (m), D_{mi} is the arithmetic average diameter between two screens (m) and X_i is weight fraction of particle size D_{mi} (%).

Characteristic bands of chitosan and deacetylation degree (%DD) were verified through FT-IR analysis. Chitosan samples were macerated and submitted to the spectroscopic determination in the infra-red ray region (Prestige 21, the 210045, Japan) using the technique of diffuse reflectance in potassium bromide (Sakkayawong et al., 2005). Deacetylation degree was determined according to Eq. (3) (Cervera et al., 2004):

$$\%DD = 87.8 - \left[3\frac{A_{C=O}}{A_{-OH}}\right] \quad (3)$$

where $A_{C=O}$ is the absorbance of CO group, A_{-OH} is the absorbance of –OH group and %DD is the deacetylation degree (%).

Chitosan powder before and after the adsorption process was characterized by scanning electron microscopy (SEM) (Jeol, JSM-6060, Japan) (Chatterjee et al., 2007) and energy dispersive X-ray spectroscopy (Pioneer, S2 Ranger, Germany) (Moghaddam, Moghaddam, & Arami, 2010).

2.3. Adsorbate

Two food dyes were used in this study, the azo dye food yellow 3 (color index 15985, molar weight $452.4\ g\,mol^{-1}$) and the triarylmethane dye acid blue 9 (color index 42090, molar weight $792.8\ g\,mol^{-1}$) (Plury chemical Ltd., Brazil). The food dyes chemical structures are presented in Fig. 1. All the other reagents utilized were of analytical-reagent grade. Distilled water was used to prepare all solutions.

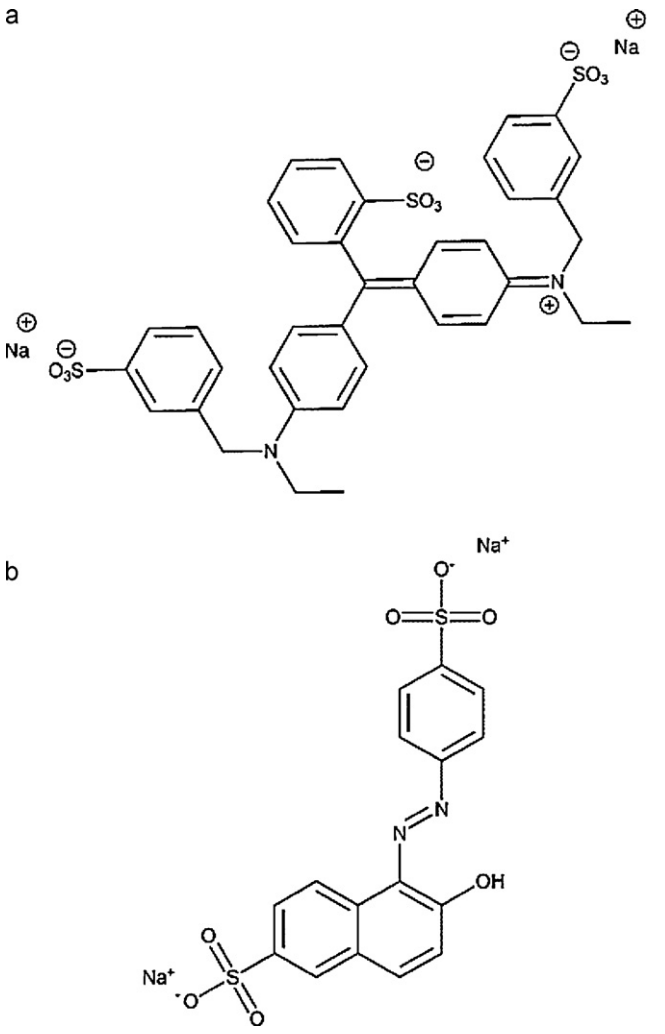

Fig. 1. The chemical structures of (a) acid blue 9 and (b) food yellow 3.

2.4. Batch experiments

Chitosan powder samples (250 mg, dry basis) were diluted in 0.80 L of distilled water and had the pH corrected (pH 3, 4 and 5) through the 50 mL of buffer disodium phosphate/citric acid solution ($0.1\ mol\,L^{-1}$), which did not present interaction with the dyes. The solutions were agitated for 30 min so that the pH reached equilibrium, which was measured before and after the adsorption process (Mars, MB10, Brazil). 50 mL of a solution containing $2\ g\,L^{-1}$ of dyes was added to each chitosan solution, being completed to 1 L with distilled water, thus, the initial dye concentration was approximately $100\ mg\,L^{-1}$ (Piccin et al., 2009).

The experiments were carried out in a jar test (Nova ética, 218 MBD, Brazil), under agitation (50 rpm, 150 rpm and 250 rpm) and ambient temperature ($25 \pm 1\ ^{\circ}C$). Aliquots were withdrawn in preset time intervals (20 min, 40 min and 60 min), and the dye concentration was found by means of spectrophotometer (Quimis, Q108 DRM, Brazil) at 408 nm and 480 nm for acid blue 9 and food yellow 3, respectively. All experiments were carried out in replicate.

The adsorption capacity (q), valid when the solute remaining in the liquid filling the pores is negligible, was determined according to Eq. (4) (Crini & Badot, 2008):

$$q = \frac{C_0 - C_t}{m} V \quad (4)$$

Table 1
Experimental design and results according to the 3^3 full factorial design.

Experiment	pH	Stirring rate (rpm)	Contact time (min)	q acid blue 9 (mg g^{-1})[a]	q food yellow 3 (mg g^{-1})[a]
1	3	50	20	105.6 ± 0.5	237.5 ± 1.0
2	3	50	40	165.8 ± 1.0	272.8 ± 2.2
3	3	50	60	144.0 ± 0.7	294.5 ± 2.4
4	3	150	20	134.3 ± 0.9	197.7 ± 0.6
5	3	150	40	181.7 ± 1.2	266.8 ± 0.3
6	3	150	60	209.9 ± 3.0	250.6 ± 0.9
7	3	250	20	142.0 ± 2.5	207.2 ± 0.8
8	3	250	40	167.6 ± 1.0	249.2 ± 1.9
9	3	250	60	175.3 ± 2.0	246.5 ± 1.4
10	4	50	20	86.3 ± 0.2	200.9 ± 2.5
11	4	50	40	124.8 ± 0.7	219.9 ± 2.0
12	4	50	60	124.8 ± 1.7	232.1 ± 1.2
13	4	150	20	58.6 ± 0.2	154.3 ± 0.8
14	4	150	40	107.3 ± 1.0	184.1 ± 0.6
15	4	150	60	135.5 ± 0.4	203.1 ± 0.5
16	4	250	20	47.1 ± 0.8	157.0 ± 2.3
17	4	250	40	140.7 ± 2.1	185.5 ± 1.7
18	4	250	60	133.0 ± 2.0	192.2 ± 0.5
19	5	50	20	59.4 ± 2.3	141.3 ± 2.8
20	5	50	40	88.9 ± 0.4	179.2 ± 2.4
21	5	50	60	54.3 ± 0.8	188.7 ± 1.2
22	5	150	20	80.4 ± 0.3	17.3 ± 1.9
23	5	150	40	115.0 ± 0.9	77.0 ± 0.5
24	5	150	60	86.8 ± 0.6	45.8 ± 0.9
25	5	250	20	50.9 ± 0.2	115.0 ± 0.5
26	5	250	40	152.2 ± 1.4	115.0 ± 0.2
27	5	250	60	50.9 ± 0.5	162.4 ± 2.0

[a] Mean ± stantard error in replicate.

where C_0 is the initial dye concentration in liquid phase (mg L^{-1}), C_t is the dye concentration in liquid phase at time t (mg L^{-1}), m is chitosan amount (g), q is the adsorption capacity (mg g^{-1}) and V is the volume of solution (L).

2.5. Statistical analysis

The influence of the variables (pH, stirring rate and contact time) on adsorption capacity was studied employing a 3^3 full factorial design (Myers & Montgomery, 2002). Runs were performed at random. Experimental range and levels of the independent process variables are shown in Table 1. Results were analyzed using Statistica version 7 (StatSoft Inc., USA) software. The statistical significance of the regression coefficients was determined by Student's test, the second order model equation was evaluated by Fischer's test and the proportion of variance explained by the model obtained was given by the multiple coefficient of determination, R^2.

2.6. Kinetics analysis

In the optimal condition of the adsorption process, experiments were carried out in order to obtain kinetic data (The experiments were carried out in the same way as of Section 2.4, however, aliquots were removed at 2, 4, 6, 8, 10, 15, 20, 25, 30, 40, 60, 80, 100 and 120 min.). All experiments were performed in replicate. In order to elucidate adsorption kinetic, the pseudo-first order, pseudo-second order and Elovich models were fitted to experimental data.

The pseudo-first order and pseudo-second order kinetic models assume that the adsorption is a pseudo-chemical reaction, and adsorption rate can be determined, respectively, for the pseudo-first, Eq. (5), and pseudo-second order, Eq. (6), equations (Qiu, Pan, Zhang, Zhang, & Zhang, 2009):

$$q_t = q_1(1 - \exp(-k_1 t)) \quad (5)$$

$$q_t = \frac{t}{(1/k_2 q_2^2) + (t/q_2)} \quad (6)$$

where q_t is the adsorption capacity at time (min) 't' (mg g^{-1}), q_1, q_2 and q_t (mg g^{-1}) are the adsorption capacities at equilibrium, k_1(min^{-1}) and k_2(g mg^{-1} min^{-1}) are the pseudo-first and pseudo-second order rate constants.

When the adsorption processes involves chemiosorption in solid surface, and the adsorption velocity decreases with the time due to covering of the superficial layer, the Elovich model, Eq. (7), is one of the most used (Wu, Tseng, & Juang, 2009).

$$q_t = \frac{1}{a}\ln(1 + abt) \quad (7)$$

where "a" is considered the initial velocity due to ($dq/dt = a$) with $q_t = 0$ (mg g^{-1} min^{-1}) and b is the desorption constant of the Elovich model (g mg^{-1}).

The coefficient's values of the kinetic equations were determined from fit of the models to the experimental data by nonlinear regression, using the software Statistica 7.0 (StatSoft Inc., USA), its fit were verified through the correlation coefficient (R^2) and average relative error (E) (Eq. (8)):

$$E = \frac{100}{n}\sum_l^n \frac{q_{t,\mathrm{exp}} - q_{t,\mathrm{obs}}}{q_{t,\mathrm{obs}}} \quad (8)$$

where $q_{t,\mathrm{exp}}$ and $q_{t,\mathrm{obs}}$ are the experimental values of adsorption capacity in time "t" and obtained from kinetics models.

3. Results and discussion

3.1. Chitosan characterization

Chitosan showed M_w 147 ± 5 kDa and particle size of 70 ± 5 μm. The FT-IR analysis was realized (figures are not shown) and were observed peaks in 1556 cm^{-1} (–NH$_2$), 1640 cm^{-1} (amide I band), 1020 cm^{-1} and 1080 cm^{-1} (C–N), 2933 cm^{-1} (N–H). These peaks are involved in the functional group of amine on chitosan polymer. In addition, in 3470 cm^{-1} the hydroxyl groups linked in the chitosan structure were observed. In acid conditions, chitosan amino and hydroxyl groups are responsible for dye adsorption (Crini & Badot, 2008). Chitosan %DD obtained from FT-IR analysis was 85 ± 1%.

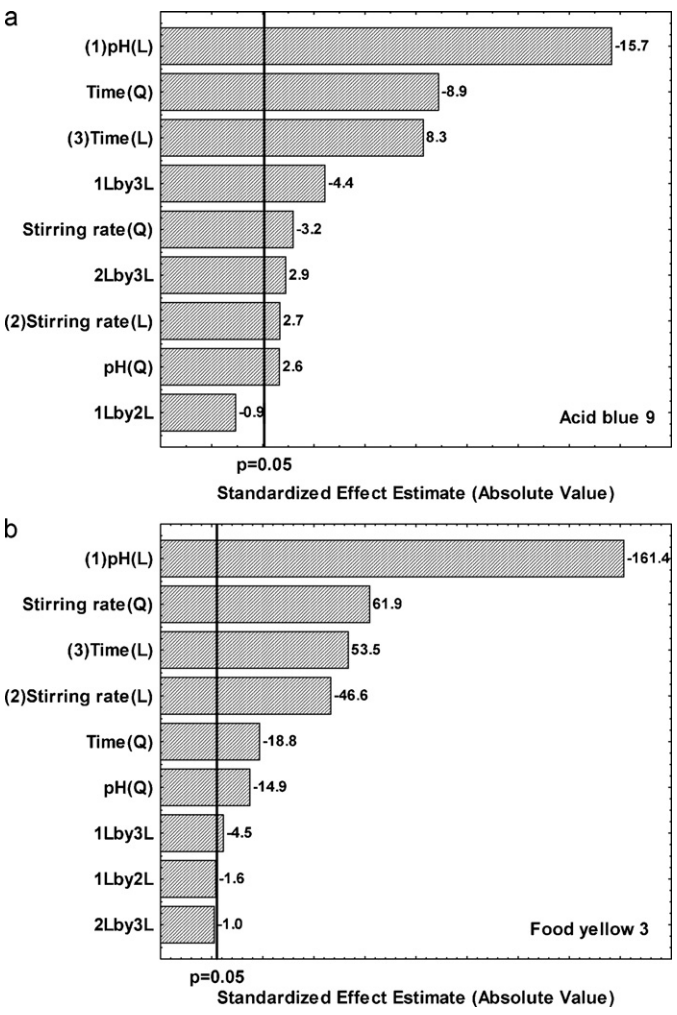

Fig. 2. Pareto charts of (a) acid blue 9 adsorption capacity and (b) food yellow 3 adsorption capacity.

3.2. Optimization of food dyes adsorption

The experimental design and results according to the 3^3 full factorial design were shown in Table 1.

Pareto chart (Fig. 2) was used in order to verify the significance of pH, stirring rate, contact time and its interactions in adsorption capacity. In Fig. 2(a) it can be observed that for the acid blue 9 adsorption capacity, the linear effects of pH, stirring rate and contact time were significant ($p \leq 0.05$). A quadratic effect of the pH, contact time and stirring rate were significant ($p \leq 0.05$). For food yellow 3 adsorption capacity (Fig. 2(b)), all main linear and quadratic effects were significant ($p \leq 0.05$).

Eqs. (9) and (10) show adsorption capacity of the acid blue 9 and food yellow 3 respectively onto chitosan as a function of pH (x_1), stirring rate (x_2) and contact time (x_3). The non significant terms ($p > 0.05$) were removed from the equations.

$$q_{acid} = 139.7 + 10.5x_1^2 - 12.6x_2^2 - 35.1x_3^2 - 35.9x_1 + 6.1x_2 + 18.9x_3 - 12.3x_1x_3 + 8.4x_2x_3 \quad (9)$$

$$q_{food} = 171.2 - 10.5x_1^2 + 43.5x_2^2 - 13.2x_3^2 - 65.5x_1 - 18.9x_2 + 21.7x_3 - 2.3x_1x_3 \quad (10)$$

Analysis of variance and Fischer *F*-test of the models (Eqs. (9) and (10)) were carried out in order to verify the models prediction and significance. The acid blue 9 adsorption model (Eq. (9)) was significant and predictive, calculated Fischer, ($F_{calc} = 19.9$) is ten times superior in relation to standard Fischer ($F_{std} = 2.2$) and coefficient of determination $R^2 = 0.92$. Similar behavior was observed for the food yellow 3 adsorption model (Eq. (10)), calculated Fischer ($F_{calc} = 73.2$) is twenty times superior in relation to ($F_{std} = 2.5$) and coefficient of determination $R^2 = 0.95$. Thus, response surfaces based in the models were used to represent adsorption capacities. Fig. 3(a) shows response surface of acid blue 9 adsorption capacity and Fig. 3(b) shows response surface of food yellow 3 adsorption capacity.

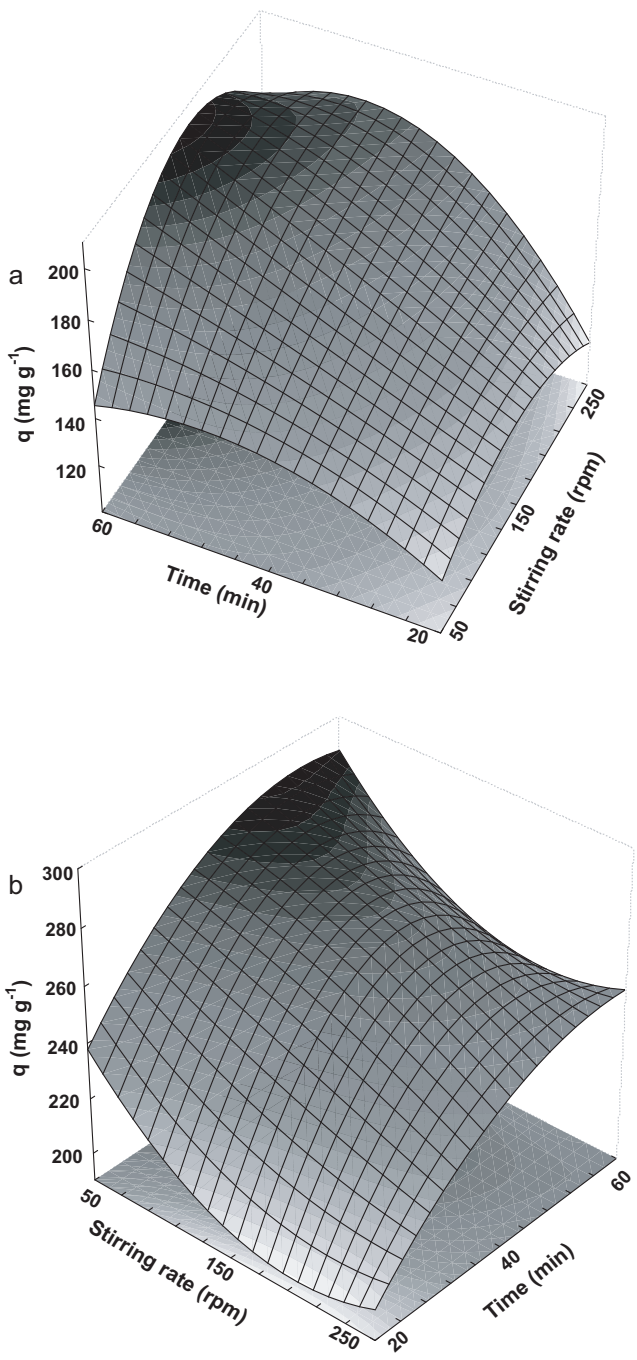

Fig. 3. Response surfaces that represents (a) acid blue 9 adsorption capacity and (b) food yellow 3 adsorption capacity as a function of stirring rate (x_2) and contact time (x_3) according to Eqs. (9) and (10), respectively.

The response surfaces (Fig. 3) are presented in pH 3, because, for both dyes, negative strong linear effect of the pH showed that

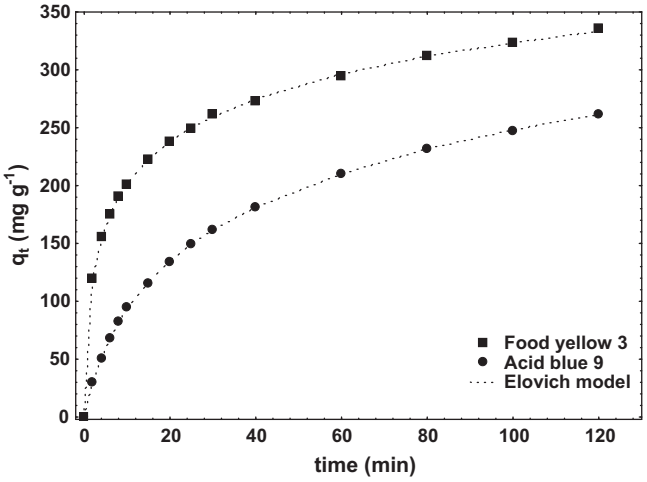

Fig. 4. Adsorption kinetics of acid blue 9 (●) and food yellow 3 (■) in the optimal conditions. (- - -) Elovich model.

pH decrease caused an increase in adsorption capacity (Fig. 2). This behavior can be explained due to the dye–chitosan interactions in acid conditions proposed by Stefancich, Delben, and Muzzarelli (1994). Under acidic conditions, hydrogen atoms (H^+) in the solution could protonate the amine groups ($-NH_2$) of chitosan, in addition, acid blue 9 and food yellow 3 were dissolved and its sulfonate groups were dissociated, the adsorption process then proceeded due to the electrostatic interactions between dyes sulfonated groups and chitosan protonated amino groups. The pH decrease caused protonation of more chitosan amino groups, increasing adsorption sites, and consequently increasing adsorption capacity. A similar behavior was observed by Cheung et al. (2009) in acid dye adsorption on chitosan nanoparticles. In this research pH increase from 4 to 6 decreased adsorption capacity ten-fold. According to Crini and Badot (2008) an optimal range for dye adsorption onto chitosan is from 3 to 6, and below this range, usually a large excess of competitor anions limits adsorption efficiency.

In Fig. 3 it can be observed that a contact time effect is similar for both dyes. The dye adsorption capacity increased with contact time, reaching the equilibrium in about 60 min. This behavior can be explained because during the process, chitosan surface was progressively blocked by the dyes reaching pseudo-equilibrium in about 60 min. According to Crini and Badot (2008), generally, the adsorption capacity increases with time and, at some point in time, reaches a constant value where no more dye is removed from the solution. At this point, the dye amount being adsorbed onto the material is in a state of dynamic equilibrium with the dye amount desorbed from the adsorbent. Similar behavior was found by Gibbs et al. (2003) in adsorption of acid green 25 onto chitosan, when, 1–2 h was sufficient to achieve complete recovery of the dye at initial concentrations below 100 mg L^{-1}. Kamari, Ngah, and Liew (2009) showed that optimum agitation period for the adsorption of acid red 37 and acid blue 25 onto chitosan and chitosan-EGDE beads were 100 and 140 min, respectively.

The stirring rate showed different behavior for each dye. For the acid blue 9 adsorption, the stirring rate showed a quadratic behavior reaching the maximum adsorption capacity at about 150 rpm (Fig. 3(a)). When stirring rate increased from 50 rpm to 150 rpm, chitosan boundary-layer resistance decreased and system mobility increased, increasing the adsorption capacity. From 150 rpm to 250 rpm, adsorption capacity decreased. This behavior can be explained due to the fact that chitosan–dye interactions are chemical and physical (Chatterjee et al., 2007), so a high stirring speed causes a break in physical chitosan–dye intermolecular interactions decreasing adsorption capacity. On the other hand, in the food yellow 3 adsorption (Fig. 3(b)) the stirring rate increase from 50 rpm to 150 rpm occurred a decrease in adsorption capacity, after 150 rpm, the stirring rate showed a small effect. The maximum value was reached in 50 rpm. Uzun (2006) observed that the increase of stirring rate caused an increase in adsorption capacity of reactive yellow 2, but the author verified an inverse behavior for adsorption of reactive blue 5. This shows that two behaviors are possible.

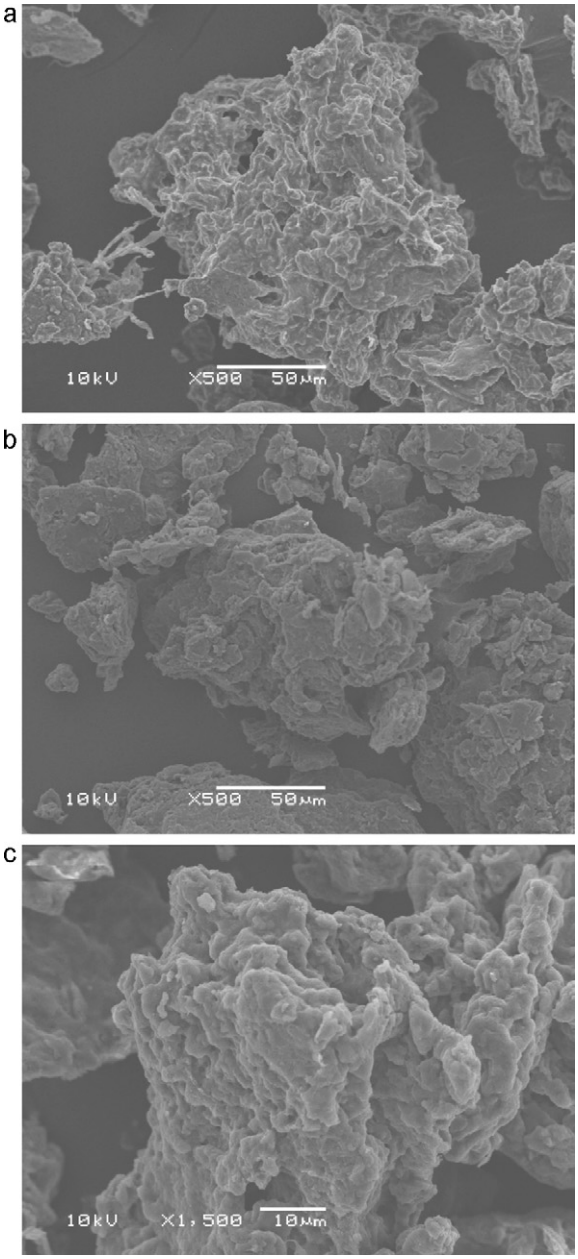

Fig. 5. Scanning electron micrographs (SEM): (a) chitosan before adsorption process, (b) chitosan adsorbed with acid blue 9 and (c) chitosan adsorbed with food yellow 3.

The optimal conditions for food dyes adsorption onto chitosan were obtained determining the maximum point of surface responses (Fig. 3). This way, the optimal process conditions for adsorption of acid blue 9 onto chitosan were pH 3, 60 min and 150 rpm, under this conditions adsorption capacity was 210 mg g^{-1}. The optimal process conditions for adsorption of food yellow 3 onto chitosan were pH 3, 60 min and 50 rpm, under

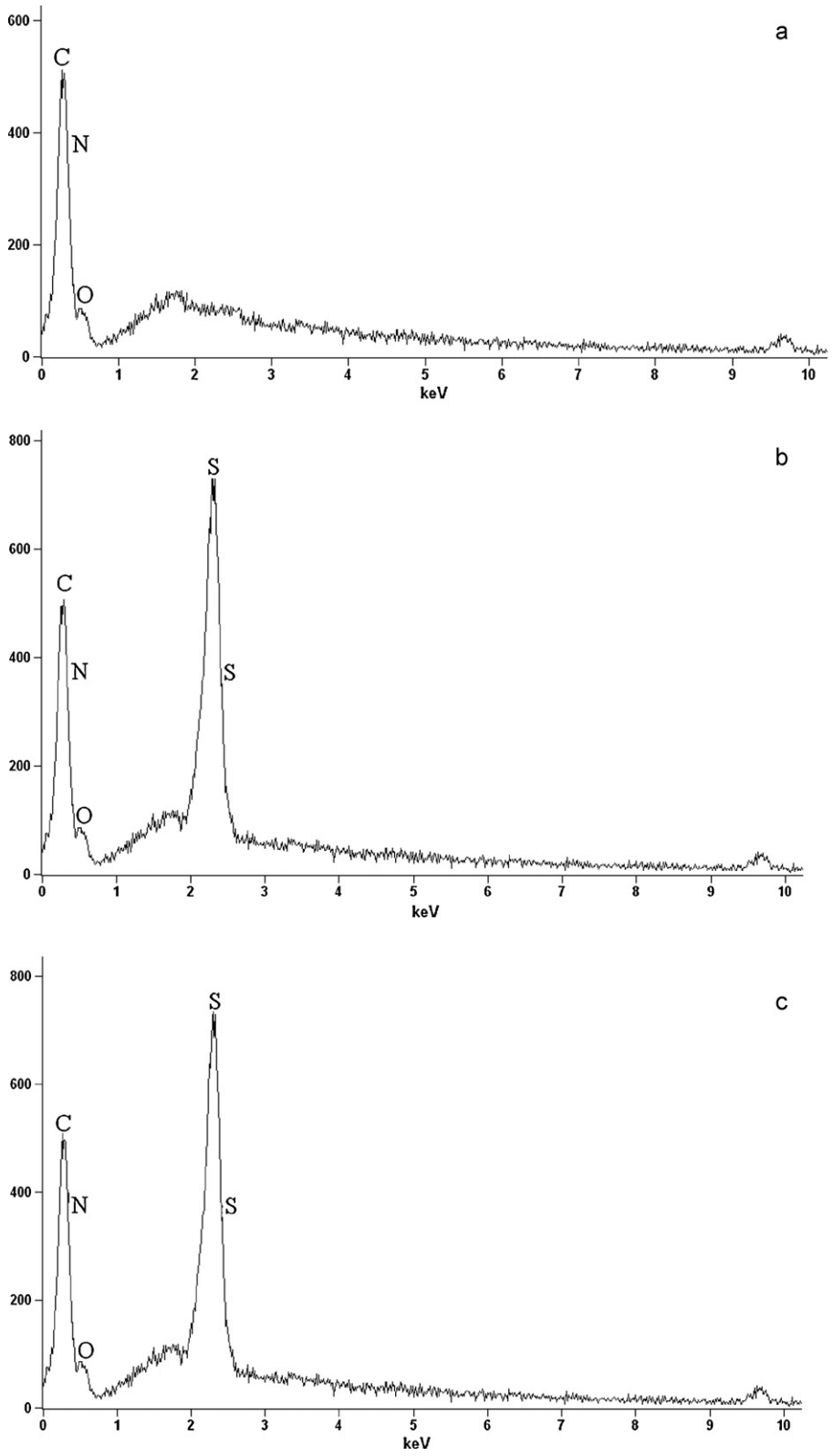

Fig. 6. Energy dispersive X-ray spectrum (EDS): (a) chitosan before adsorption process, (b) chitosan adsorbed with acid blue 9 and (c) chitosan adsorbed with food yellow 3.

this condition adsorption capacity was 295 mg g^{-1}. The adsorption capacity of acid blue 9 was lower than food yellow 3. This occurs because acid blue 9 molar weight is higher than food yellow 3 molar weight, and acid blue 9 is more ramified, so, leading to a difficulty in dye diffusion. This behavior was observed by Cestari, Vieira, Santos, Mota, and Almeida (2004) in adsorption of anionic dyes on chitosan beads. In this study they show that dimensions of the dye organic chains, amount and positioning of the sulfonate groups of the dyes influence dye adsorption by chitosan. The adsorption capacities reached in this work are in the range found in literature for dye adsorption onto chitosan. This range varies from 30 to 2500 mg g^{-1} (Crini & Badot, 2008).

Table 2
Kinetics models constants to the adsorption of acid blue 9 and food yellow 3 in the optimal condition.

Kinetic model	Acid blue 9	Food yellow 3
Pseudo-first-order		
k_1 (min^{-1})	0.040	0.137
q_1 ($mg\,g^{-1}$)	245.2	289.7
E (%)	11.4	12.0
R^2	0.965	0.893
Pseudo-second-order		
k_2 ($\times 10^4\,g\,mg^{-1}\,min^{-1}$)	1.5	5.8
q_2 ($mg\,g^{-1}$)	297.3	322.6
E (%)	5.7	6.7
R^2	0.985	0.972
Elovich		
a ($\times 10^3\,mg\,g^{-1}\,min^{-1}$)	12.9	18.7
b ($g\,mg^{-1}$)	18.2	224.7
E (%)	0.4	0.4
R^2	0.999	0.999

3.3. Kinetic analysis

In the optimal condition for each dye, adsorption kinetics was investigated. Fig. 4 shows adsorption kinetics of acid blue 9 and food yellow 3 in this condition.

In Fig. 4, the kinetic curves showed that for both dyes, adsorption was fast, reaching about 85% of saturation in 60 min. Later, adsorption rate decreased considerably. Fast kinetic is characteristic in dye–chitosan systems and is desirable in wastewater treatment because it provides high adsorption capacities in short times. The kinetics models constants, coefficients of determination and average relative error are shown in Table 2.

In Table 2, the low values of average relative error ($E < 0.5\%$) and the high values of coefficients of determination ($R^2 > 0.99$) show that the Elovich model was the best to represent adsorption kinetic of both dyes onto chitosan. This suggests that adsorption of both dyes onto chitosan was controlled by chemiosorption, and chitosan was covered by superficial layer of the dyes. Similar behavior was obtained by Wu et al. (2009) in adsorption of reactive red 222 onto chitosan. In their work Elovich model was the best to represent kinetic experimental data, indicating a chemical interaction of dye–chitosan.

In order to compare adsorption behavior of both dyes, SEM and EDS were carried out in chitosan before and after adsorption process. Fig. 5 shows chitosan before adsorption process, chitosan adsorbed with acid blue 9, and chitosan adsorbed with food yellow 3. SEM of chitosan before adsorption process, Fig. 5(a), showed that the surface of unadsorbed chitosan was a typically wrinkled polymeric network with irregular pores. In addition a heterogeneous surface area and porous internal structure were observed. After adsorption of acid blue 9, (Fig. 5(b)), chitosan pores were not visible. This shows that a dye thin layer has covered the entire external chitosan surface. In chitosan adsorbed with food yellow 3, (Fig. 5(c)), the dye had densely and homogeneously adhered to the chitosan surface.

Energy dispersive X-ray spectrum (EDS) of chitosan before adsorption process, chitosan adsorbed with acid blue 9 and chitosan adsorbed with food yellow 3 are showed in Fig. 6.

The results of EDS analysis from an average of scanned points showed that the elements of chitosan particles are: C, N and O (Fig. 6(a)). After adsorption process (Fig. 6(b) and (c)), the appearance of S can be observed, due to the trapped dye molecules which contain sulphonic groups, indicating a chemical interaction of dye–chitosan. The EDS analysis suggest that the adsorption of acid blue 9 and food yellow 3 onto chitosan proceeded due to the electrostatic interactions between dyes sulfonated groups and chitosan protonated amino groups.

4. Conclusion

In this research, food dyes adsorption onto chitosan was optimized. The optimal process conditions for the acid blue 9 adsorption were pH 3, 60 min and 150 rpm, and for the food yellow 3 adsorption were pH 3, 60 min and 50 rpm. In these conditions, adsorption capacities values were 210 $mg\,g^{-1}$ and 295 $mg\,g^{-1}$, for acid blue 9 and food yellow 3, respectively.

In the optimal condition, adsorption kinetic was evaluated. The Elovich kinetic model was the best in order to represent experimental data ($R^2 > 0.99$ and $E < 0.5\%$). This indicates that chitosan surface was covered by food dyes and adsorption occurred by chemiosorption. SEM and EDS analysis indicated the chitosan surface coverage and interaction between the sulphonate group of the dyes and the amino group of the chitosan.

Acknowledgements

The authors would like to thank CAPES (Brazilian Agency for Improvement of Graduate Personnel) and CNPq (National Council of Science and Technological Development) for the financial support.

References

Cervera, M. F., Heinamaki, J., Rasanem, M., Maunu, S. L., Karjalainen, M., Acosta, O. M. N., et al. (2004). Solid state characterization of chitosan derived from lobster chitin. *Carbohydrate Polymers*, *58*, 401–408.

Cestari, A. R., Vieira, E. F. S., Santos, A. G. P., Mota, J. A., & Almeida, V. P. (2004). Adsorption of anionic dyes on chitosan beads. 1. The influence of the chemical structures of dyes and temperature on the adsorption kinetics. *Journal of Colloid and Interface Science*, *280*, 380–386.

Chatterjee, S., Chatterjee, S., Chatterjee, B. P., & Guha, A. K. (2007). Adsorptive removal of Congo red, a carcinogenic textile dye by chitosan hydrobeads: Binding mechanism, equilibrium and kinetics. *Colloids and Surfaces A: Physicochemical and Engineering Aspects*, *299*, 146–152.

Cheung, W. H., Szeto, Y. S., & McKay, G. (2009). Enhancing the adsorption capacities of acid dyes by chitosan nano particles. *Bioresource Technology*, *100*, 1143–1148.

Crini, G., & Badot, P. M. (2008). Application of chitosan, a natural aminopolysaccharide, for dye removal from aqueous solutions by adsorption processes using batch studies: A review of recent literature. *Progress in Polymer Science*, *33*(4), 399–447.

Elwakeel, K. Z. (2009). Removal of Reactive Black 5 from aqueous solutions using magnetic chitosan resins. *Journal of Hazardous Materials*, *167*, 383–392.

Foust, A. S., Wenzel, L. A., Clump, C. W., Maus, L., & Andersen, L. B. (1980). *Principles of unit operations* (2nd ed.). New York: John Wiley & Sons.

Gibbs, G., Tobin, J. M., & Guibal, E. (2003). Adsorption of acid green 25 on chitosan: Influence of experimental parameters on uptake kinetics and adsorption isotherms. *Journal of Applied Polymer Science*, *90*, 1073–1080.

Gupta, V. K., & Suhas. (2009). Application of low-cost adsorbents for dye removal—A review. *Journal of Environmental Management*, *90*, 2313–2342.

Halal, C. Y., Moura, J. M., & Pinto, L. A. A. (2010). Evaluation of molecular weight of chitosan in thin-layer and spouted bed drying. *Journal of Food Process Engineering*, 2010. doi:10.1111/j.1745-4530.2008.00345.x

Han, R., Zhang, L., Song, C., Zhang, M., Zhu, H., & Zhang, L. (2010). Characterization of modified wheat straw, kinetic and equilibrium study about copper ion and methylene blue adsorption in batch mode. *Carbohydrate Polymers*, *79*, 1140–1149.

Harish Prashanth, K. V., & Tharanathan, R. N. (2007). Chitin/chitosan: Modifications and their unlimited application potential an overview. *Trends in Food Science & Technology*, *18*, 117–131.

Kamari, A., Ngah, W. S. W., & Liew, L. K. (2009). Chitosan and chemically modified chitosan beads for acid dyes sorption. *Journal of Environmental Science*, *21*, 296–302.

Li, G., Du, Y., Tao, Y., Deng, H., Luo, X., & Yang, J. (2010). Iron(II) cross-linked chitin-based gel beads: Preparation, magnetic property and adsorption of methyl orange. *Carbohydrate Polymers*, *82*, 706–713.

Moghaddam, S. S., Moghaddam, M. R. A., & Arami, M. (2010). Coagulation/flocculation process for dye removal using sludge from water treatment plant: Optimization through response surface methodology. *Journal of Hazardous Materials*, *175*, 651–657.

Myers, R. H., & Montgomery, D. C. (2002). *Response surface methodology: Process and product optimization using designed experiments* (2nd ed.). New York: John Wiley & Sons.

Piccin, J. S., Vieira, M. L. G., Gonçalves, J., Dotto, G. L., & Pinto, L. A. A. (2009). Adsorption of FD&C Red No. 40 by chitosan: Isotherms analysis. *Journal of Food Engineering*, *95*, 16–20.

Qiu, H., Pan, L. L., Zhang, Q. J., Zhang, W., & Zhang, Q. (2009). Critical review in adsorption kinetic models. *Journal of Zhejiang University Science*, *10*, 716–724.
Sakkayawong, N., Thiravetyan, P., & Nakbanpote, W. (2005). Adsorption mechanism of synthetic reactive dye wastewater by chitosan. *Journal of Hazardous Materials*, *145*(1), 250–255.
Shimei, X., Jingli, W., Ronglan, W., & Jide, W. (2006). Effect of degree of substitution on adsorption behavior of Basic Green 4 by highly crosslinked amphoteric starch with quaternary ammonium and carboxyl groups. *Carbohydrate Polymers*, *66*, 55–59.
Srinivasan, A., & Viraraghavan, T. (2010). Decolorization of dye wastewaters by biosorbents: A review. *Journal of Environmental Management*, *91*, 1915–1929.
Stefancich, S., Delben, F., & Muzzarelli, R. A. A. (1994). Interactions of soluble chitosans with dyes in water I. Optical evidence. *Carbohydrate Polymers*, *24*, 17–23.
Uzun, I. (2006). Kinetics of the adsorption of reactive dyes by chitosan. *Dyes and Pigments*, *70*, 76–83.
Weska, R. F., Moura, J. M., Batista, L. M., Rizzi, J., & Pinto, L. A. A. (2007). Optimization of deacetylation in the production of chitosan from shrimp wastes: Use of response surface methodology. *Journal of Food Engineering*, *80*, 749–753.
Wu, F. C., Tseng, R. L., & Juang, R. S. (2009). Characteristics of Elovich equation used for the analysis of adsorption kinetics in dye chitosan systems. *Chemical Engineering Journal*, *150*, 366–373.
Zhang, H., & Neau, S. H. (2001). In vitro degradation of chitosan by a commercial enzyme preparation: Effect of molecular weight and degree of deacetylation. *Biomaterials*, *22*, 1653–1658.
Zhao, H., Zhang, M., & Zeng, A. (2003). Research on chitosan degradation by H_2O_2 oxidation method. *Chemical Industrial Engineering Progress*, *2*, 160–164.